

RSC Advances



This is an *Accepted Manuscript*, which has been through the Royal Society of Chemistry peer review process and has been accepted for publication.

Accepted Manuscripts are published online shortly after acceptance, before technical editing, formatting and proof reading. Using this free service, authors can make their results available to the community, in citable form, before we publish the edited article. This *Accepted Manuscript* will be replaced by the edited, formatted and paginated article as soon as this is available.

You can find more information about *Accepted Manuscripts* in the [Information for Authors](#).

Please note that technical editing may introduce minor changes to the text and/or graphics, which may alter content. The journal's standard [Terms & Conditions](#) and the [Ethical guidelines](#) still apply. In no event shall the Royal Society of Chemistry be held responsible for any errors or omissions in this *Accepted Manuscript* or any consequences arising from the use of any information it contains.

ARTICLE

Facile Synthesis of Nitrogen-doped Carbon Derived from Polydopamine Coated $\text{Li}_3\text{V}_2(\text{PO}_4)_3$ as Cathode Materials for Lithium-Ion Batteries

Cite this: DOI: 10.1039/x0xx00000x

Cunliang Zhang,^{a, b} Hongshen Li,^a Nie Ping,^a Gang Pang,^a Guiyin Xu,^a Xiaogang Zhang*^aReceived 00th January 2012,
Accepted 00th January 2012

DOI: 10.1039/x0xx00000x

www.rsc.org/

Nitrogen-doped carbon coated $\text{Li}_3\text{V}_2(\text{PO}_4)_3$ cathode materials were prepared by the oxidative self-polymerization of dopamine on $\text{Li}_3\text{V}_2(\text{PO}_4)_3$ surface and subsequent carbonization of polydopamine. Field emission scanning electron microscopy (FESEM), scanning transmission electron microscopy-energy dispersive X-ray spectroscopy (STEM-EDS) and X-ray photoelectron spectroscopy (XPS) were performed to characterize their morphologies and structures. The uniform nitrogen-doped carbon coating provided a continuous electronic conducting network. Furthermore, the existence of nitrogen in the composite can improve the electronic conductivity. As cathode materials for lithium ions batteries, the nitrogen-doped carbon-coated $\text{Li}_3\text{V}_2(\text{PO}_4)_3$ composites display superior rate performance and excellent cycle performance over the pristine $\text{Li}_3\text{V}_2(\text{PO}_4)_3$ and carbon-coated $\text{Li}_3\text{V}_2(\text{PO}_4)_3$. The electrode delivers high specific capacity of 74 mAh g^{-1} at 10 C, and still remains of 95.4% of the initial capacity after 100 cycles at 1 C.

Introduction

With the increasing concerns about environmental issues caused by conventional energy, there has been an urgent demand to develop renewable and clean energy sources [1-2]. Recently, lithium-ion batteries (LIBs) have been widely used in portable electronic devices, transportation, and storage of renewable energy for smart grid due to its high energy density. However, LIBs suffer from some deficiencies, including low power density, poor cycling performance and poor safety that hinder their large-scale application [3-5]. Therefore, the search for efficient electrode materials especially with enhanced lithium storage properties is emerging [6-9].

In fact, cathode materials determined energy density, safety and life cycle of lithium-ion batteries [10]. Up to now, layered transition metal oxides, spinel-type oxides and polyanion cathode materials have been investigated intensively as potential cathode materials. Layered transition metal oxides have several advantages: fully developed synthetic routes, high capacity and facile processing. Nevertheless, they all have a drawback, namely oxygen evolution at high charging potential, which could cause serious safety issues for practical application. Spinel-type oxides such as LiMn_2O_4 have the advantages of thermal stability, low cost and environmental friendliness. However, they suffer fast capacity fading during cycling, especially at elevated temperatures. Polyanion materials have attracted tremendous attention as cathodes for LIBs owing to their robust structure, low cost and high voltage plateau [6, 7, 11]. In particular, monoclinic lithium vanadium phosphate, $\text{Li}_3\text{V}_2(\text{PO}_4)_3$, one of the phosphate compounds with sodium super ionic conductor (NASICON) framework has been considered as a promising cathode material due to its high

operating voltage, large theoretical specific capacity, structural stability and abundant reserves [12-14]. However, the poor electronic conductivity ($2.4 \times 10^{-7} \text{ S cm}^{-1}$) of $\text{Li}_3\text{V}_2(\text{PO}_4)_3$ due to the separated VO_6 octahedra arrangement hinders its practical application. Carbon coating is an effective way to improve electrochemical performance, because it improves the surface electronic conductivity and the electric contact between particles and conducting agents [13,14]. Recently, $\text{Li}_3\text{V}_2(\text{PO}_4)_3/\text{C}$ nanosphere cathode with three-dimensional conductive network was synthesized, where the 3D structure effectively enhanced the electron transport and the electrochemical performance [17]. Duan and co-workers reported a hydrothermal-assisted sol-gel method to prepare the $\text{Li}_3\text{V}_2(\text{PO}_4)_3@\text{C}$ core-shell nanocomposite, which exhibited remarkably high rate capability and long cyclability [18]. The introduction of nitrogen into a carbon structure can tune the carbon properties, because it fabricates more active defects which show higher Li^+ diffusion efficiency compared with conventional carbon coating [19-22].

Dopamine (2-(3,4-dihydroxyphenyl)ethylamine), a nitrogenous nature-inspired biomimetic material, which contains catechol and amine functional groups, can self-polymerize and deposit on virtually any surface [23-27]. Thus polydopamine has opened a new route to modify electrode materials and stimulated extensive research [28-34]. The polyethylene separator properties were dramatically improved by simple immersion into the dopamine solution [28]. Polydopamine was also used as binder for silicon anode to substantially improve the electrochemical properties due to its unique wetness-resistant adhesion [29]. Nitrogen-doped carbon-coated $\text{Li}_4\text{Ti}_5\text{O}_{12}$ microspheres were used as anode material which displayed superior rate performance and excellent

capacity retention [30]. The anatase TiO₂ nanoparticles with the carbon coating derived from polydopamine were reported [32]. Kong et al. reported the enhanced electrochemical properties of SnO₂-based anodes prepared by in situ polymerization of dopamine [33].

In this paper, a facile method was proposed for the synthesis of Li₃V₂(PO₄)₃ composite with a carbon coating structure by using dopamine as a nitrogen-doped carbon precursor. The nitrogen-doped carbon shell as a conductive network is beneficial for lithium ion transport and electric conductivity across the interface between the active materials and the electrolyte. The LVP/NC exhibits excellent high rate performance as well as superior cyclability compared with pristine Li₃V₂(PO₄)₃ and Li₃V₂(PO₄)₃/C.

Experimental

Synthesis of pristine Li₃V₂(PO₄)₃ (LVP)

All of the reactants and solvents were analytical grade and used without further purification. The LVP was prepared *via* a sol-gel route reported by Zhou's group with minor modifications [35]. In a typical procedure, pristine LVP was synthesized using Li₂CO₃, V₂O₅, NH₄H₂PO₄ and oxalic acid, as starting materials with a Li : V : P : oxalic acid molar ratio of 3:2:3:3. Stoichiometric V₂O₅ and oxalic acid were dissolved in deionized water at 70 °C to form a blue transparent aqueous solution. Then NH₄H₂PO₄ and Li₂CO₃ in a stoichiometric ratio were added to the solution with continuous stirring until a gel formed. Finally, the gel was decomposed at 350 °C in nitrogen atmosphere for 4 h, followed by sintering at 750 °C for 4h.

Synthesis of nitrogen-doped carbon coated Li₃V₂(PO₄)₃ (LVP/NC)

Typically, 200 mg LVP was dispersed in the tris-buffer (50 mL, pH=8.5) by ultrasonication for 30 min to form a suspension. Subsequently, certain amounts of dopamine were added to the suspension with constantly stirred for 6 h at room temperature. Then the precipitate was collected by centrifugation, washed several times with deionized water, and then dried at 60 °C in an electric oven for 12 h. Finally the powder was annealed in a tube under N₂ atmosphere at 750 °C for 4 h. In order to indicate the modification effects of the nitrogen doped carbon coating accurately, a comparative experiment of carbon coated Li₃V₂(PO₄)₃(LVP/C) was carried out (see Electronic Supporting Information) [36].

Material characterization

The crystal structure of the obtained samples was characterized by X-ray diffraction (XRD) (Bruker D8 advance) with Cu K α radiation. Elemental analysis was carried out by Heraeus CHN-O-Rapid. The X-ray photoelectron spectroscopy (XPS) analysis was performed on a Perkin-Elmer PHI 550 spectrometer with Al K α (1486.6 eV) as the X-ray source. The microstructure properties were observed by scanning transmission electron microscopy-energy dispersive X-ray spectroscopy (STEM-EDS, JEM-2100, JEOL), and field emission scanning electron microscopy (FESEM, JEOL, JSM-7000).

Electrochemical measurements

Electrochemical characterization was carried out by galvanostatic cycling in CR2016-type coin cells which were

assembled in an argon filled glove box. The working electrodes were formed by mixing 80 wt% active materials, 10 wt% carbon black, 10wt% polyvinylidene fluoride (PVDF) dissolved in N-methyl pyrrolidinone (NMP) and uniformly pasting the mixture on an aluminum foil current collector. Finally, the electrodes were dried at 110 °C for 12 h in vacuum oven. Lithium metal was used as both the counter and reference electrode, and the polypropylene membrane (Celgard 2400) was served as separator. The electrolyte was a 1 M solution of LiPF₆ dissolved in ethylene carbonate (EC)/dimethyl carbonate (DMC) with a volume ratio of 1:1. Galvanostatic charge/discharge experiments were performed at different current densities between 3 and 4.3 V (vs. Li/Li⁺) by using a CT2001A cell test instrument (LAND Electronic Co.). Electrochemical impedance spectra (EIS) were measured on an electrochemical workstation (CHI750D). EIS measurements were performed over a frequency range of 100 kHz to 0.01Hz with an amplitude of 5 mV. All the measurements were carried out at room temperature.

Results and discussion

The schematic of the synthesis of LVP/NC is illustrated in Fig. 1. Firstly, the LVP was prepared by a typical sol-gel route. The as-synthesized LVP, mixed with dopamine, was dispersed in the tri-buffer (pH=8.5). Through the spontaneous oxidative polymerization of dopamine on the surface of the LVP, the LVP/polydopamine was achieved. Finally, LVP/NC was obtained *via* carbonization of polydopamine by the calcination under an inert atmosphere.

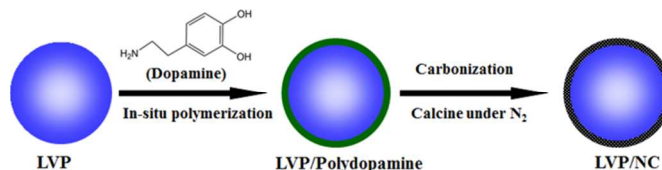


Fig.1 Schematic illustration of the synthesis of LVP/NC composites.

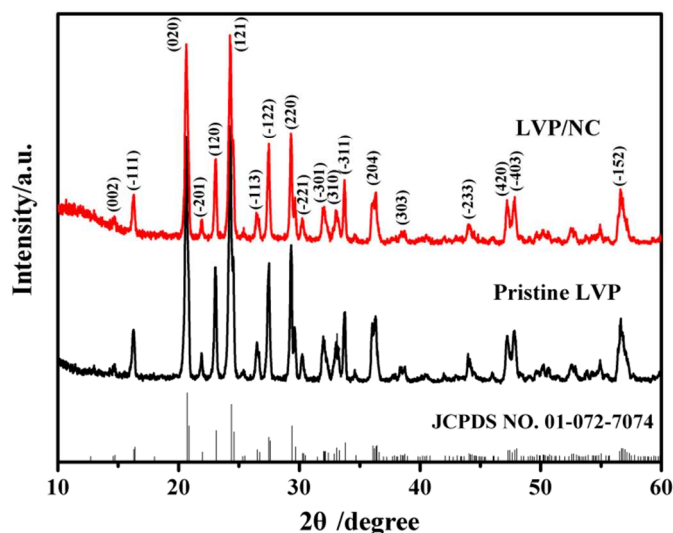


Fig. 2 XRD patterns of pristine LVP and LVP/NC.

The X-ray diffraction (XRD) patterns of the as-synthesized pristine LVP and LVP/NC are presented in Fig. 2. The major

identified peaks at $2\theta = 16.3, 20.6, 23.0, 24.3, 27.5, 29.3, 36.2, 44.0, 47.2, 47.8$ and 56.6° correspond to the (-111), (020), (120), (121), (-122), (220), (204), (-233), (420), (-403) and (-152) planes of a monoclinic lithium vanadium phosphate phase (space group: $P2_1/n$, JCPDS No. 01-072-7074) without any discernable impurities such as Li_3PO_4 , and V_2O_5 , conforming well to the previously reported literature [7,15-18]. The characteristic peak of the graphitized carbon is not detected in the pattern of LVP/NC, indicating that carbon obtained from polydopamine is amorphous. Furthermore, the carbon and nitrogen contents in the composite were 2.61 % and 0.18 %, respectively, according to elemental analysis. While the carbon content in the LVP/C was 2.7 %, according to the thermogravimetric (TG) analysis (Fig. S1).

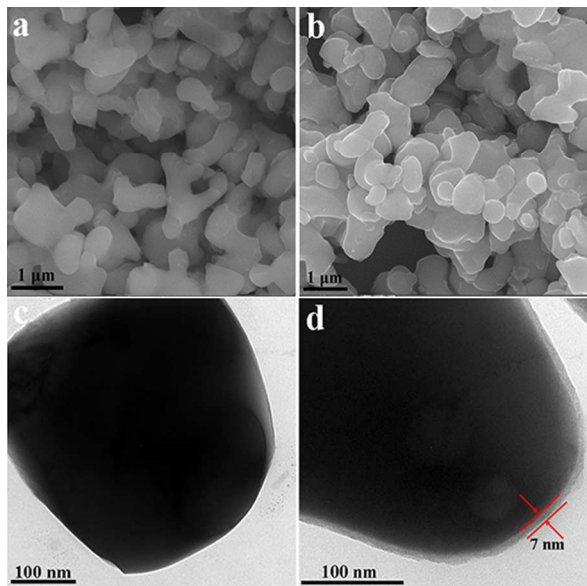


Fig. 3 SEM images of the pristine LVP (a) and LVP/NC (b), TEM images of the pristine LVP (c) and LVP/NC (d).

Fig. 3a shows the scanning electron microscopy (SEM) image of the as-synthesized pristine LVP sample, which consists of nearly spherical particles with a diameter of approximately 400 nm. Compared with the other synthesized LVP *via* solid-state reaction or sol-gel method [37, 38], the particles display better homogeneity, which is beneficial for contact between particles and electrolyte. Transmission electron microscopy (TEM) examination reveals that the surface of pristine LVP is very smooth (Fig. 3c). As can be seen from the SEM (Fig. 3b) and TEM (Fig. 3d) images, the LVP/NC composite has the same overall morphology as pristine LVP except for the uniform and continuous carbon coating. Fig. 3d shows that LVP is uniformly coated with a *ca.* 7 nm thin carbon layer, displaying a typical core-shell nanostructure, which is beneficial to enhance electronic conductivity and facilitate the electrochemical performance of the composite electrode [39].

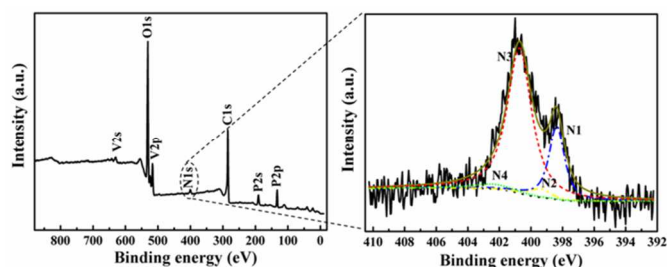


Fig. 4 XPS spectra of LVP/NC.

The XPS survey spectra of LVP/NC are shown in Fig. 4a and 4b. The peak at around 399 eV can be ascribed to N 1s in the LVP/NC survey spectra, suggesting the presence of N in LVP/NC samples [40]. From the high-resolution XPS spectrum of N 1s for LVP/NC, the N1s region exhibits three main contributions: the peak at 398.4 eV can be ascribed to pyridinic nitrogen (N1), the peak at 399.4 eV corresponds to pyrrolic nitrogen (N2), and the peak at 400.7 eV is assigned to graphite nitrogen (N3). The minor N 1s peak at 402.5 eV (N4) indicates the presence of the N-oxide of pyridinic nitrogen. XPS survey spectrum indicates that polydopamine was transformed into nitrogen-doped carbon through carbonization which is beneficial for Li^+ transport in the interface due to defects in the carbon caused by nitrogen-doping [41]. The nitrogen content measured by XPS was 2 atom%.

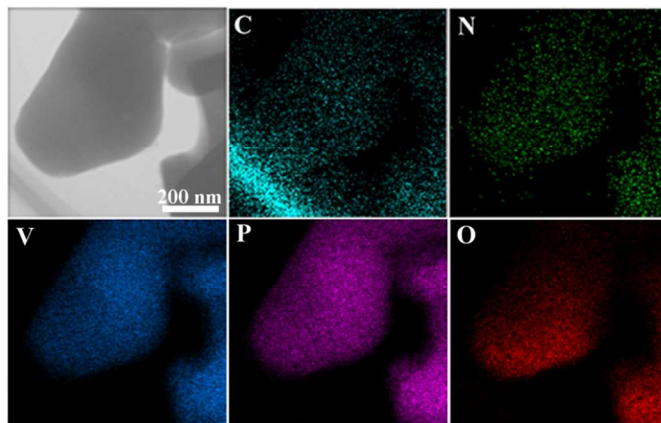


Fig. 5 The EDX mapping images of LVP/NC.

To further investigate the element distribution in the LVP/NC composite, energy dispersive X-ray (EDX) mapping was shown in Fig. 5. It can be seen that the images were overlapped with each other, which indicates that C and N distribute uniformly through the LVP sample. Both XPS and EDX analysis confirm the existence of nitrogen in the composite which can improve the electronic conductivity due to the hybridization of nitrogen lone pair electrons with the p electrons in carbon [42]. Furthermore, nitrogen-doped carbon has more defects in the graphite structure [20, 39, 43]. Hence, lithium ion can easily diffuse from the carbon shell to the LVP core.

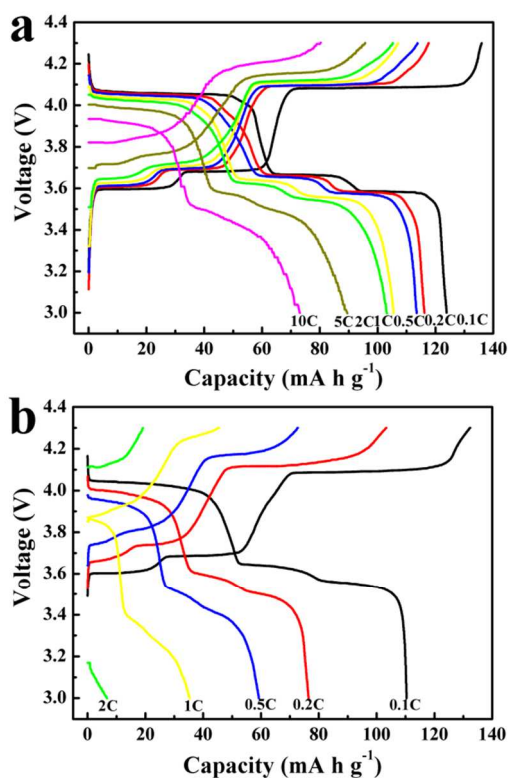


Fig. 6 Charge-discharge curves for LVP/NC (a) and LVP (b) over a potential window of 3–4.3 V. 7.6

The typical discharge-charge voltage profiles of the LVP/NC electrode at different current rates over a potential window of 3–4.3 V are shown in Fig. 6a. At the initial lower rate of 0.1 C, during the charge process, the sample showed three charge plateaus around 3.6, 3.7 and 4.1 V, which corresponded to a sequence of phase transition processes of $\text{Li}_3\text{V}_2(\text{PO}_4)_3 \rightarrow \text{Li}_{2.5}\text{V}_2(\text{PO}_4)_3 \rightarrow \text{Li}_2\text{V}_2(\text{PO}_4)_3 \rightarrow \text{LiV}_2(\text{PO}_4)_3$. Accordingly, three discharge flat plateaus could be discovered at 4.0, 3.7 and 3.6 V, which was identified as the two-phase transition processes during the electrochemical reactions. At the initial lower rate of 0.1 C, the LVP/NC samples gave a discharge capacity of 124 mAh g^{-1} , which was close to its theoretical capacity of 133 mAh g^{-1} . Moreover, with the increase of discharge-charge rate, the discharge plateau voltages decreased slightly and the electrochemical plateaus became undistinguished due to the increase of cell polarization at high current rates [44]. In Fig. 6b and Fig. S2, both LVP and LVP/C samples show the similar plateaus, but deliver lower discharge capacity of 111 mAh g^{-1} and 122 mAh g^{-1} at 0.1 C, respectively. Furthermore, the electrochemical plateau voltages of LVP and LVP/C at various current rates were also lower. These results imply that LVP/NC has the lower polarization and fast reaction kinetics during charge/discharge [45].

Rate performance of the LVP/NC, LVP and LVP/C electrodes were also evaluated (Fig. 7 and Fig. S3). The LVP/NC electrode showed the smaller capacity decay compared with LVP and LVP/C with the increase of rate. It was noteworthy that the capacity (74 mAh g^{-1}) obtained by LVP/NC at a rate of 10 C is higher than that at a rate of 0.5C for the pristine LVP. At any discharge rate, the discharge capacity of LVP/NC was always higher than LVP and LVP/C. Even when the rate was turned back to 0.1 C, a discharge capacity of 113 mAh g^{-1} (as

high as 91 % of initial capacity for LVP/NC) could be retained, much higher than that of 68 mAh g^{-1} for LVP and 109 mAh g^{-1} for LVP/C. These results indicate that LVP/NC electrode has a remarkable rate capability.

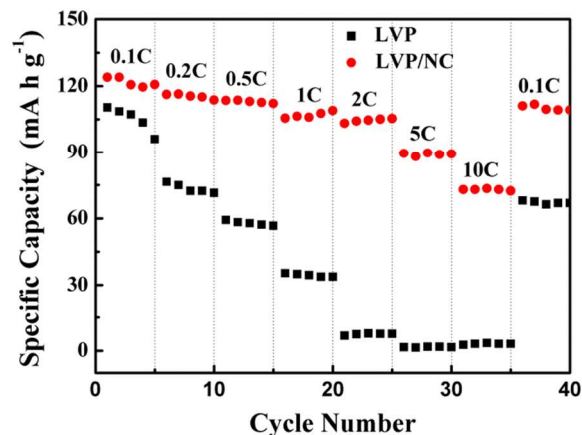


Fig. 7 The rate performances of the LVP/NC and LVP samples at different current rates over a potential window of 3–4.3 V.

The LVP/NC electrode also revealed excellent cycling performance. Fig. 8 and Fig. S4 show the cycling performances of the LVP/NC, LVP and LVP/C at 1 C between the voltage limits of 3.0–4.3 V. For the LVP/NC electrode, the initial discharge capacity was 109 mAh g^{-1} at the rate of 1C, after 100 cycles with 4.6 % capacity loss, but for LVP and LVP/C, the corresponding values were 16 mAh g^{-1} and 42.9 %, 100 mAh g^{-1} and 7.6 %. The Coulombic efficiency of the LVP/NC remained approximately 100%, which indicates that the electrochemical Li^+ insertion-extraction process is reversible even at high rates. These results further confirm the advantage of nitrogen-doped carbon as a shell for LVP electrodes.

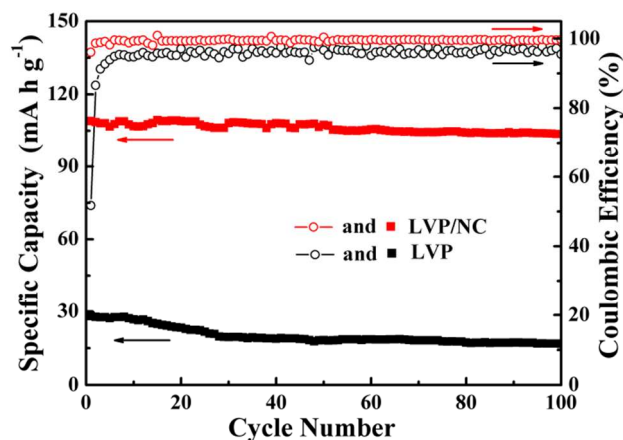


Fig. 8 The cyclability and Coulombic efficiency of the LVP/NC and LVP samples at a rate of 1 C.

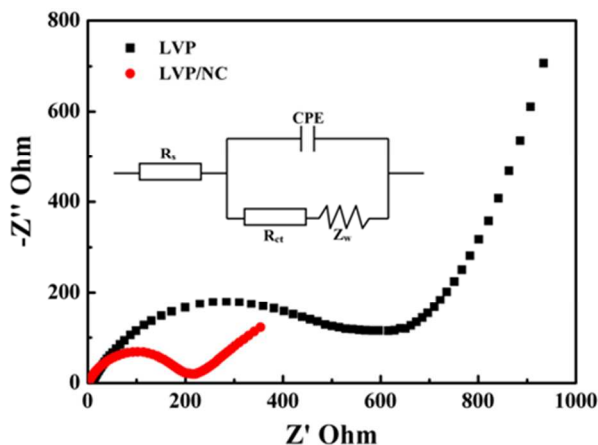


Fig.9 EIS spectra for LVP and LVP/NC with the frequency range of 100 kHz to 0.01Hz after five full cycles at 0.1 C respectively.

In order to gain insight into the remarkable rate performance of LVP/NC, we carried out AC impedance spectra measurements. As demonstrated in Fig.9 and Fig. S4, Nyquist plots spectra of electrodes exhibit a semi-circle in the high-frequency range and an inclined line in the low-frequency range. The high frequency region featuring the semicircle is attributed to the electrochemical reaction resistance and the double layer capacity of the electrode, while the low frequency region of the straight line corresponds to the diffusion of lithium ions into the bulk of the cathode material, the so-called Warburg diffusion. The fitting results were obtained by ZView software which was set using an equivalent circuit. As can be seen from the equivalent circuit, R_s and R_{ct} are the uncompensated bulk resistance (total resistance of the electrolyte, separator and electrical contact) and charge-transfer resistance, respectively. CPE is the constant phase angle element, involving double layer capacitance, and Z_w represents the Warburg impedance related to the diffusion of lithium ions into the bulk electrodes [46]. As shown in Table 1 and Table S1, the values of the charge-transfer resistance (R_{ct}) is 172 Ω for LVP/NC, which are significantly lower than those of LVP (521 Ω) and LVP/C (266 Ω), indicating that nitrogen-doped carbon coating largely enhance the electrochemical activity of LVP/NC [17, 29].

Table 1 Various resistances of LVP/NC and LVP cells after five full cycles at 0.1 C respectively.

Samples	$R_s(\Omega)$	$R_{ct}(\Omega)$
LVP	6.88	521
LVP/NC	1.85	172

Conclusions

In summary, a facile approach has been developed to synthesize LVP/NC composites. The amorphous carbon layer derived from polydopamine formed a continuous electronic conducting network which could effectively improve the electronic conductivity of the materials. Moreover, the defects in the nitrogen-doped carbon coating also provide Li^+ diffusion paths. Consequently, the resultant LVP/NC exhibits improved lithium storage properties, including high rate capability and excellent

cycle stability. At a current rate of 10 C, LVP/NC delivered a discharge capacity of 74 mAh g^{-1} . Furthermore, the capacity retention of was up to 95.1% of its initial capacity with nearly ignored capacity fading after 100 cycles at 1.0 C. In addition to the application of the LVP/NC, we anticipate that the versatile synthetic approach could be extended to modify other electrode materials for high-performance energy storage devices.

Acknowledgements

This work was supported by the National Basic Research Program of China (973Program) (No.2014CB239701), National Natural Science Foundation of China (No. 21173120, 51372116), Natural Science Foundation of Jiangsu Province (BK2011030), the Fundamental Research Funds for the Central Universities (NP2014403).

Notes and references

^a College of Material Science & Engineering and Key Laboratory for Intelligent Nano Materials and Devices of Ministry of Education, Nanjing University of Aeronautics and Astronautics, Nanjing, 210016, PR China. E-mail: azhangxg@163.com.

^bShangqiu Polytechnic, Shangqiu, 476000, PR China

- J.B. Goodenough, and K.S. Park, *J. Am. Chem. Soc.*, 2013, **135**, 1167.
- B. Dunn, H. Kamath, J.M. Tarascon, *Science*, 2011, **334**, 928.
- M. Armand, and J.M. Tarascon, *Nature*, 2008, **451**, 652.
- K.S. Park, A. Benayad, D.J. Kang, and S.G. Doo, *J. Am. Chem. Soc.*, 2008, **130**, 14930.
- P.G. Bruce, B. Scrosati, and J.M. Tarascon, *Angew. Chem. Int. Ed.*, 2008, **47**, 2930.
- C. Masquelier, and L. Croguennec, *Chem. Rev.*, 2013, **113**, 6552.
- Q.L. Wei, Q.Y. An, D.D. Chen, L.Q. Mai, S.Y. Chen, Y.L. Zhao, K.M. Hercule, L. Xu, A. Minhas-khan, and Q.J. Zhang, *NanoLett.*, 2014, **14**, 1042.
- L.F. Shen, H.S. Li, E. Uchaker, X.G. Zhang, and G.Z. Cao, *NanoLett.*, 2012, **12**, 5673.
- L.F. Shen, H.S. Li, E. Uchaker, X.G. Zhang, and G.Z. Cao, *Adv. Mater.*, 2012, **24**, 6502.
- M. Tarascon and M. Armand, *Nature*, 2001, **414**, 359.
- Z. L. Gong and Y. Yang, *Energy Environ. Sci.*, 2011, **4**, 3223.
- J. Kim, J.K. Yoo, Y.S. Jung, and K. Kang, *Adv. Energy Mater.*, 2013, **3**, 1004.
- H. Huang, S.C. Yin, T. Kerr, N. Taylor, and L.F. Nazar, *Adv. Mater.*, 2002, **14**, 1525.
- S.C. Yin, H. Grondey, P. Strobel, M. Anne, and L. Nazar, *J. Am. Chem. Soc.*, 2003, **125**, 10402.
- Z.Y. Chen, H.Z. Jin, C.S. Dai, G. Wu, M. Nelson, and Y.F. Chen, *Int. J. Electrochem. Sci.*, 2013, **8**, 8153.
- Y.Z. Li, Z. Zhou, X.P. Gao, and J. Yan, *Electrochim. Acta*, 2007, **52**, 4922.
- L.Q. Mai, S. Li, Y.F. Dong, Y.L. Zhao, Y.Z. Luo, and H.M. Xu, *Nanoscale*, 2013, **5**, 4864.
- W.C. Duan, Z. Hu, K. Zhang, F.Y. Cheng, and Z.L. Tao, *Nanoscale*, 2013, **5**, 6485.
- W.H. Shin, H.M. Jelong, B.G. Kim, J.K. Kang, and J.W. Choi, *NanoLett.* 2012, **12**, 2283.

- 20 Z.J. Ding, L. Zhao, L.M. Suo, Y. Jiao, S. Meng, Y.S. Hu, Z.X. Wang, and L.Q. Chen, *Phys. Chem. Chem. Phys.*, 2011, **13**, 15127.
- 21 C. Wang, W. Shen, and H. M. Liu, *New J. Chem.*, 2014, **38**, 430
- 22 J.P. Paraknowitsch, A. Thomas, and M. Antonietti, *J. Mater. Chem.*, 2010, **20**, 6746.
- 23 H. Lee, S.M. Dellatore, W.M. Miller, and P.B. Messersmith, *Science*, 2007, **318**, 426.
- 24 R. Liu, S.M. Mahurin, C.Li, R. Unocic, J.C. Idrobo, H. Gao, S.J. Pennycook, and S. Dai, *Angew. Chem. Int. Ed.*, 2011, **50**, 6799.
- 25 A. Postma, Y. Yan, Y. Wang, A.N. Zelikin, E. Tjpto, and F. Caruso, *Chem. Mater.*, 2009, **21**, 3042.
- 26 J.H. Jiang, L.P. Zhu, L.J. Zhu, B.K. Zhu, and Y.Y. Xu, *Langmuir*, 2011, **27**, 14180.
- 27 Y.L.Liu, K.L. Ai, and L.H. Lu, *Chem. Rev.*, 2014, **114**, 5057.
- 28 M.H. Ryou, Y.M. Lee, J.K. Park, and J.W. Choi, *Adv. Mater.*, 2011, **23**, 3066.
- 29 M.H. Ryou, J.Kim, I.Lee, S. Kim, Y.K. Jeong, S. Hong, J.H. Ryu, T.S. Kim, J.K. Park, H. Lee, and J.W. Choi, *Adv. Mater.*, 2013, **25**, 1571.
- 30 H.S. Li, L.F. Shen, K.B. Yin, J. Ji, J. Wang, X.Y. Wang, and X.G. Zhang, *J. Mater. Chem.A*, 2013, **1**, 7270.
- 31 Z.X. Chi, W. Zhang, F.Q. Cheng, J.T. Chen, A.M. Cao, and L.J. Wan, *RSC Adv.*, 2014, **4**, 7795.
- 32 L. Tan, P. Lei, C.Y. Cao, B.F. Wang, and L. Li, *J. Power Sources*, 2014, **253**, 193.
- 33 J.H. Kong, W.A. Yee, L.P. Yang, Y.F. Wei, S.L. Phua, H.G. Ong, J.M. Ang, X. Li, and X.H. Lu, *Chem. Commun.*, 2012, **48**, 10316.
- 34 C. Lei, F. Han, D. Li, W.C. Li, Q. Sun, X.Q. Zhang, and A.H. Lu, *Nanoscale*, 2013, **5**, 1168.
- 35 M.M. Ren, Z. Zhou, X.P. Gao, W.X. Peng, and J.P. Wei, *J. Phys. Chem. C*, 2008, **14**, 5689.
- 36 X. M. Sun, and Y. D.Li, *Angew. Chem. Int. Ed.*, 2004, **43**, 597
- 37 C.S. Dai, Z.Y. Chen, H.Z. Jin, and X.G. Hu, *J. Power Sources*, 2010, **195**, 5775.
- 38 Y.Z. Li, Z. Zhou, M.M. Ren, X.P. Gao, and J. Yan, *Electrochim. Acta*, 2006, **51**, 6498.
- 39 C.X. Wang, G.J. Shao, Z.P. Ma, S. Liu, W. Song, and J.J. Song, *Electrochim. Acta*, 2014, **130**, 679.
- 40 H.S. Li, L.F. Shen, J. Wang, B. Ding, P. Nie, G.Y. Xu, X.Y. Wang, and X.G. Zhang, *ChemPlusChem*, 2014, **79**, 128.
- 41 Z.J. Ding, L. Zhao, L.M. Suo, Y. Jiao, S. Meng, Y.S. Hu, Z.X. Wang, and L.Q. Chen, *Phys. Chem. Chem. Phys.*, 2011, **13**, 15127.
- 42 N.Y. Wang, C.H. Shih, P.T. Chiueh, and Y.F. Huang, *Energies*, 2013, **6**, 871.
- 43 C.C. Ma, X.H. Shao, and D.P. Cao, *J. Mater. Chem.*, 2012, **22**, 8911.
- 44 D.L. Li, M. Tian, R. Xie, Q. Li, X.Y. Fan, P. Zhao, S.L. Ma, Y.X. Shi, H.T.H. Yong, *Naonoscale*, 2014, **6**, 3302.
- 45 H.S. Li, L.F. Shen, X.G. Zhang, J. Wang, P. Nie, Q. Che, and B. Ding, *J. Power Sources*, 2013, **221**, 122.
- 46 S.B. Yang, X.L. Feng, and K. Müllen, *Adv. Mater.*, 2011, **23**, 3575.